Received: 30 July 2022 | Revised: 11 November 2022 | Accepted: 3 December 2022

DOI: 10.1111/bph.16005

RESEARCH ARTICLE

Non-neuronal TRPA1 encodes mechanical allodynia associated with neurogenic inflammation and partial nerve injury in rats

Francesco De Logu[1] | Gaetano De Siena[1] | Lorenzo Landini[1] | Matilde Marini[1] | Daniel Souza Monteiro de Araujo[1] | Valentina Albanese[2] | Delia Preti[3] | Antonia Romitelli[1] | Martina Chieca[1] | Mustafa Titiz[1] | Luigi F. Iannone[1] | Pierangelo Geppetti[1] | Romina Nassini[1]

[1]Department of Health Sciences, Clinical Pharmacology and Oncology Section, University of Florence, Florence, Italy

[2]Department of Environmental and Prevention Sciences - DEPS, University of Ferrara, Ferrara, Italy

[3]Department of Chemical, Pharmaceutical and Agricultural Sciences, University of Ferrara, Ferrara, Italy

Correspondence
Pierangelo Geppetti, Department of Health Sciences, Clinical Pharmacology and Oncology Section, University of Florence, Florence 50139, Italy.
Email: geppetti@unifi.it

Funding information
H2020 European Research Council, Grant/Award Number: 835286

Background and Purpose: The pro-algesic transient receptor potential ankyrin 1 (TRPA1) channel, expressed by a subpopulation of primary sensory neurons, has been implicated in various pain models in mice. However, evidence in rats indicates that TRPA1 conveys nociceptive signals elicited by channel activators, but not those associated with tissue inflammation or nerve injury. Here, in rats, we explored the TRPA1 role in mechanical allodynia associated with stimulation of peptidergic primary sensory neurons (neurogenic inflammation) and moderate (partial sciatic nerve ligation, pSNL) or severe (chronic constriction injury, CCI) sciatic nerve injury.

Experimental Approach: Acute nociception and mechanical hypersensitivity associated with neurogenic inflammation and sciatic nerve injury (pSNL and CCI) were investigated in rats with TRPA1 pharmacological antagonism or genetic silencing. TRPA1 presence and function were analysed in cultured rat Schwann cells.

Key Results: Hind paw mechanical allodynia (HPMA), but not acute nociception, evoked by local injection of capsaicin or allyl isothiocyanate, the TRP vanilloid 1 (TRPV1) or the TRPA1 activators was mediated by CGRP released from peripheral sensory nerve terminals. CGRP-evoked HPMA was sustained by a ROS-dependent TRPA1 activation, probably in Schwann cells. HPMA evoked by pSNL, but not that evoked by CCI, was mediated by ROS and TRPA1 without the involvement of CGRP.

Conclusions and Implications: As found in mice, TRPA1 mediates mechanical allodynia associated with neurogenic inflammation and moderate nerve injury in rats. The channel contribution to mechanical hypersensitivity is a common feature in rodents and might be explored in humans.

KEYWORDS
nerve injury, neurogenic inflammation, oxidative stress, Schwann cells, TRPA1

Abbreviations: AITC, allyl isothiocyanate; AS, antisense; CCI, chronic constriction injury; DRG, dorsal root ganglion; HPMA, hind paw mechanical allodynia; i.pl., intraplantar; pSNL, partial sciatic nerve ligation.

Francesco de Logu and Gaetano De Siena contributed equally to this work.

1 | INTRODUCTION

The **transient receptor potential (TRP)** family of channels encompasses several nonselective cation channels expressed in a variety of cells, including a subpopulation of primary sensory neurons, where they encode sensory modalities that span from thermosensation to mechanical and chemical stimuli (De Logu & Geppetti, 2019; Story et al., 2003; Talavera et al., 2020). Major attention has been paid to the **TRP vanilloid 1 (TRPV1)**, also known as the capsaicin (hot pepper) receptor, and the **TRP ankyrin 1 (TRPA1)**, also known as the **allyl isothiocyanate (AITC**, a spicy component of wasabi of wasabi) receptor (Szallasi & Blumberg, 1999; Talavera et al., 2020). TRPV1 and TRPA1 are abundantly expressed in a heterogeneous subpopulation of primary sensory neurons that consists of peptidergic and non-peptidergic C-fibre and Aδ-fibre nociceptors (Bhattacharya et al., 2008). TRPV1 and TRPA1 stimulation results in the release of the neuropeptides, **substance P (SP)** and **calcitonin gene-related peptide (CGRP**; Nassini et al., 2014), which elicit plasma protein extravasation and adhesion of leukocytes to postcapillary venules (mediated by SP) and arteriolar vasodilatation (mediated by CGRP), collectively referred to as neurogenic inflammation (Geppetti & Holzer, 1996). **Capsaicin**, acting on TRPV1, is the prototypical agent that evokes sensory neuropeptide release and neurogenic inflammation (Szallasi & Blumberg, 1999). Capsaicin injection in the mouse and human skin also elicits an acute and transient nociceptive response or pain respectively, and in both species a sustained mechanical hypersensitivity (De Logu et al., 2022; LaMotte et al., 1992) that in mice is mediated by CGRP (De Logu et al., 2022).

In recent years, the role of TRPA1 in sustaining mechanical allodynia has been identified in mouse models of inflammatory, neuropathic, cancer and migraine pain. These include intra-articular injection of monosodium urate (Trevisan et al., 2014), hind limb ischemia and reperfusion (De Logu et al., 2020), partial sciatic nerve ligation (pSNL) (De Logu et al., 2017), alcoholic polyneuropathy (De Logu et al., 2019), melanoma cells inoculation (De Logu et al., 2021) and CGRP injection into the periorbital skin (De Logu et al., 2022). In addition to the contribution of neuronal TRPA1, which signals agonist-induced acute nociception, a critical role of Schwann cell TRPA1 has been identified in macrophage-dependent (De Logu et al., 2021, 2017) and macrophage-independent (De Logu et al., 2019, 2022) sustained mechanical allodynia.

Pain-like responses produced in rat models of inflammatory and neuropathic conditions have been reported to be reduced by first generation TRPA1 receptor antagonists (Eid et al., 2008; McNamara et al., 2007; Petrus et al., 2007; Wei et al., 2009), which, however, suffered from poor selectivity or suboptimal pharmacokinetics. More recently, TRPA1 deletion in rats by CRISPR technology, while attenuating acute nociception by AITC, failed to reduce mechanical hypersensitivity in models of inflammatory and neuropathic pain, such as those evoked by chronic constriction injury (CCI), the chemotherapeutic agent **bortezomib** and complete Freund adjuvant (Reese et al., 2020). These findings led to the conclusion that TRPA1 involvement in pathophysiological models of various pain states is confined to mice and cannot be replicated in other rodent species (Reese et al., 2020).

What is already known

- The TRPA1 channel has been implicated in various pain models in mice.

What does this study add

- The role of TRPA1 in mechanical allodynia has been investigated in a rat model of neurogenic inflammation and moderate/severe sciatic nerve injury.

What is the clinical significance

- TRPA1 implication in mechanical hypersensitivity is a common feature in rodents and may be explored in humans.

Here, we aimed to answering the general question as to whether the pro-algesic role of TRPA1 is limited to mice or if it can be observed in other rodent species. To this purpose, we explored whether TRPA1 is implicated in sustaining mechanical allodynia associated with neurogenic inflammation and involved in two models of neuropathic pain in rats. We found that while acute nociceptive responses elicited by AITC and capsaicin injection in the rat hind paw were dependent on their respective selective targets (TRPA1 and TRPV1, respectively), mechanical allodynia was exclusively due to CGRP release and the activation of non-neuronal TRPA1, most likely on Schwann cells, that senses, amplifies and sustains the pro-allodynic oxidative stress signal. We also confirmed that in rats the failure of TRPA1 antagonism fails to attenuate allodynia in a severe model of neuropathic pain (CCI), however TRPA1 and oxidative stress were markedly implicated in allodynia in the less severe pSNL model. Thus, TRPA1 seems to have a conserved ability to encode various pain modalities across different mammal species, including rats, in pathophysiological pain models.

2 | METHODS

2.1 | Animals

Sprague–Dawley rats (male, 150 g, Charles River, Milan, Italy, RRID: RGD_734476) were used throughout. Given that, in various previous reports in mice no gender difference was found in the pro-algesic

role of TRPA1 (De Logu et al., 2020, 2021, 2022), here, in accordance with the 3Rs guidelines to minimize animal number, we used only male rats. The group size of n = 6 animals for behavioural experiments was determined by sample size estimation using G*Power (Version 3.1.9.6-available from https://gpower.software.informer.com/3.1/) (Faul et al., 2007) to detect size effect in a post hoc test with type 1 and 2 error rates of 5 and 20%, respectively. Rats were allocated to vehicle or treatment groups using a randomization procedure (http://www.randomizer.org/). Investigators were blinded to treatments, which were revealed only after data collection. No animals were excluded from experiments. All behavioural experiments were in accordance with European Union (EU) guidelines for animal care procedures and the Italian legislation (DLgs 26/2014) application of EU Directive 2010/63/EU. Study was approved by the Italian Ministry of Health (research permit 360/2022-PR). Animal studies are reported in compliance with the ARRIVE guidelines (Percie du Sert et al., 2020) and with the recommendations made by the British Journal of Pharmacology (Lilley et al., 2020). Rats were housed in a temperature- and humidity-controlled *vivarium* (12-h dark/light cycle, free access to food and water, five animals per cage). At least 1 h before behavioural experiments, rats were acclimatized to the testing room and behaviour was evaluated between 9:00 am and 5:00 pm. All the procedures were conducted following the current guidelines for laboratory animal care and the ethical guidelines for investigations of experimental pain in conscious animals set by the International Association for the Study of Pain (Kilkenny et al., 2010). Animals were killed with inhaled CO_2 plus 10-50% O_2 and confirmation of death was achieved by a physical method of killing (decapitation) (AVMA Guidelines for the Euthanasia of Animals, 2020).

2.2 | Partial ligation of the sciatic nerve

pSNL was performed in rats as previously described (Seltzer et al., 1990). Briefly, rats were anaesthetized with a mixture of ketamine (100 mg kg^{-1}) and xylazine (10 mg kg^{-1}), placed on a heated surface to maintain body temperature and the right sciatic nerve was exposed at high-thigh level. Under a magnification of 25×, the dorsum of the nerve was carefully freed from surrounding connective tissues at a site near the trochanter just distal to the point at which the posterior bicep semitendinosus nerve branches off the common sciatic nerve. The nerve was fixed in its place by pinching the epineurium on its dorsal aspect, taking care not to press the nerve against underlying structures. A silicon treated silk suture was inserted into the nerve and tightly ligated so that the dorsal I/3-1/2 of the nerve thickness was trapped in the ligature. The wound was then closed. In sham-operated rats, used as controls, the right sciatic nerve was exposed, but not ligated. Rats were maintained in spontaneous breathing, monitored, and adequately rehydrated until fully recovered from anaesthesia. After surgery rats were maintained one per cage and fed with standard rodent chow (Envigo, Milan, Italy) and water ad libitum.

2.3 | CCI to sciatic nerve

CCI to sciatic nerve was performed as previously described (Bennett & Xie, 1988). Briefly, rats were anaesthetized with a mixture of ketamine (100 mg kg^{-1}) and xylazine (10 mg kg^{-1}) placed on a heated surface to maintain body temperature and the common sciatic nerve was exposed at the level of the middle of the thigh by blunt dissection through the bicep femoris. Proximal to the sciatic trifurcation, about 7 mm of nerve was freed of adhering tissue and four ligatures (5.0 Ethicon chromic catgut) were tied loosely around it with about 1-mm spacing. Great care was taken to tie the ligatures, such that the diameter of the nerve was seen to be just barely constricted. In sham-operated rats, used as controls, the right sciatic nerve was exposed, but not ligated. Rats were maintained in spontaneous breathing monitored, and adequately rehydrated until fully recovered from anaesthesia. After surgery rats were maintained one per cage and fed with a standard rodent chow and water ad libitum.

2.4 | Treatment protocols

Rats received unilateral (right hindpaw) intraplantar (i.pl.) injection (20 µl per site) of allyl isothiocyanate (AITC, 200 nmol solution diluted in mineral oil) or vehicle (mineral oil), capsaicin (10 nmol) or vehicle (0.5% DMSO), CGRP (1.5 nmol), SP (3.5 nmol) or vehicle (0.9% NaCl). Some rats were treated (0.5 h before or 0.5 h after the stimulus) with i.pl. (20 µl per site) **A-967079** (300 nmol), L733,060 (20 nmol), **olcegepant** (1 nmol), SQ22536 (25 nmol), **L-NAME** (1 µmol), N-tert-butyl-α-phenylnitrone (PBN, 670 nmol) or vehicle (4% DMSO 4% Tween 80 in 0.9% NaCl). Other rats received intraperitoneal (i.p., 10 ml kg^{-1}) A-967079 (10, 30 and 100 mg kg^{-1}), AMG0902 (AMG, 10, 30 and 100 mg kg^{-1}) **capsazepine** (CPZ, 4 mg kg^{-1}) or vehicle (4% DMSO 4% Tween 80 in 0.9% NaCl) before the stimulus or at day 15 after pSNL, CCI or sham surgery.

In different experiments, rats were randomly allocated to the groups receiving perineural (p.n., 10 µl) or intrathecal (i.th., 10 µl) treatment with TRPA1 antisense (AS) or mismatch (MM) oligonucleotide (ODN) (10 nmol), once a day for four consecutive days, or once a day for four consecutive days, starting from day 10 to day 14 after pSNL, CCI, or sham surgery. TRPA1 AS-oligonucleotide sequence was 5′-TATCGCTCCACATTGCTAC-3′, TRPA1 MM-oligonucleotide sequence was 5′-ATTCGCCTCACATTGTCAC-3′. Perineural injections were performed by injecting the compound into the region surrounding the sciatic nerve at high thigh level of right hind limbs without skin incision using a microsyringe fitted with a 30-gauge needle.

2.5 | Behavioural assay

2.5.1 | Acute nociception

Each rat was lightly restrained in a towel and an intraplantar injection of 20 µl was made to the right hindpaw using a 30-gauge disposable

needle attached to a luer-tipped Hamilton syringe. Immediately after the i.pl. injection, rats were placed inside a plexiglass chamber and spontaneous nociception was assessed for 10 min by measuring the time (seconds) that the animal spent licking/lifting the injected paw.

2.5.2 | Paw mechanical allodynia

Paw mechanical allodynia was evaluated by measuring the paw withdrawal threshold using the up-down paradigm (Chaplan et al., 1994; Dixon, 1980). Rats were acclimatized (1 h) in individual clear plexiglass boxes on an elevated wire mesh platform, to allow for access to the plantar surfaces of the hind paws. Von Frey filaments of increasing stiffness (0.4, 0.6, 1.0, 1.4, 2, 4,8,10 and 15 g) were applied to the hind paw plantar surfaces of rats with enough pressure to bend the filament. The absence of a paw being lifted after 5 s led to the use of the next filament with an increased force, whereas a lifted paw indicated a positive response, leading to the use of a subsequently weaker filament. Six measurements were collected for each rat or until four consecutive positive or negative responses occurred. The 50% mechanical withdrawal threshold (expressed in grams) was then calculated.

2.6 | Cell cultures

Human embryonic kidney 293T (HEK293T-#CRL-3216, RRID:CVCL_0063, American Type Culture Collection, ATCC) cells were transfected with 1 μg of the cDNA for rat TRPA1 (#RR203182, OriGene Technologies GmbH) (rTRPA1-HEK293T) using jetOPTIMUS DNA transfection reagent (Polyplus) according with manufacturer's instructions. Non-transfected HEK293T were used as control.

Rat Schwann cells were isolated from sciatic nerve of Sprague–Dawley rats (Tao, 2013). Briefly, sciatic nerve was dissected, the epineurium was removed and nerve explants were divided into 1-mm segments and dissociated enzymatically using collagenase (0.05%) and hyaluronidase (0.1%) in HBSS (2 h, 37°C). Cells were collected by centrifugation (150×*g*, 10 min, room temperature) and the pellet was resuspended and cultured in DMEM containing fetal calf serum (10%), L-glutamine (2 mM), penicillin (100 U ml^{-1}), streptomycin (100 mg ml^{-1}), neuregulin (10 nM) and forskolin (2 μM). Three days later, cytosine-b-D-arabino-furanoside free base (ARA-C, 10 mM) was added to remove fibroblasts. Cells were cultured at 37°C in 5% CO_2 and 95% O_2. Purity of primary Schwann cells cultured according to the present protocol reaches almost 100%. The culture medium was replaced every 3 days and cells were used after 15 days of culture.

For primary culture of rat dorsal root ganglia (DRG) neurons, DRGs (combined cervical, thoracic and lumbar) were bilaterally excised under a dissection microscope and enzymatically digested using 2 mg ml^{-1} of collagenase type 1A and 1 mg ml^{-1} of trypsin in 4 ml of HBSS for 35 min at 37°C. Ganglia were disrupted by several passages through a series of syringe needles (23–25G). Rat neurons were then pelleted by centrifugation at 1200× rpm for 5 min at 4°C and resuspended in DMEM supplemented with 10% heat inactivated horse serum containing 10% heat-inactivated FBS, 100 U ml^{-1} of penicillin, 0.1 mg ml^{-1} streptomycin and 2-mM L-glutamine added with 100 ng ml^{-1} nerve growth factor (NGF) and 2.5 mM ARA-C and maintained at 37°C in 5% CO_2 and 95% O_2 for 2 days before being used.

2.7 | RNAscope

Frozen tissue sections of sciatic nerve and DRG (10 μm) from naïve rats were baked for 30 min at 60°C and washed with 1× PBS. Primary culture of rat Schwann cells from naïve rats were grown on poly-L-lysine-coated (8.3 μM) 35-mm glass coverslips and maintained at 37°C in 5% CO_2 and 95% O_2 for 48 h before being dehydrated with incubation of increasing concentrations of ethanol (50-70 and 100%) and stored at −20°C in ethanol 100%. On the day of the experiment, cells were rehydrated by exposure to decreasing concentrations of ethanol (70% and 50%) and incubated 10 min at room temperature (RT) in 1× PBS.

Rat Schwann cells and sciatic nerve and DRG tissues were treated with hydrogen peroxide (#322335, ACD HybEZ™) for 10 min at RT. Target retrieval was performed for 5 min at 99–100°C and then by a treatment with Protease Plus (#322331, ACD HybEZ™) for 30 min at 40°C. Samples were subsequently hybridized with a probe specific to rat TRPA1 (#312511, ACD HybEZ™) and negative (#310043, ACD HybEZ™) control probe for 2 h at 40°C. Sequential signal amplification and red chromogenic detection was performed using RNAscope® 2.5 HD Detection kit – RED (#322360, ACD HybEZ™). After chromogen development, cells were washed in distilled water, PBS and triton X-100 (0.1%) (PBS-T), and incubated in 4% normal goat serum in PBS-T for 1-h RT. Sciatic nerve and rat Schwann cell slides were subjected to an immunofluorescent labelling using Alexa Fluor® 488 anti-S100 beta antibody [EP1576Y] (#ab196442, RRID:AB_2722596, monoclonal rabbit, 1:100, Abcam) overnight at 4°C. Both DRG and sciatic nerve sections were coverslipped using mounting medium with DAPI - Aqueous, Fluoroshield (#ab104139, Abcam). Fluorescent images were acquired using a Zeiss Axio Imager 2, Zeiss ZEN imaging 2020. The Immuno-related procedures used comply with the recommendations made by the *British Journal of Pharmacology* (Alexander et al., 2018).

2.8 | Ca^{2+} imaging

Cells were plated on poly-L-lysine-coated (8.3 μM) 35 mm glass coverslips and maintained at 37°C in 5% CO_2 and 95% O_2 for 24 h. Cells were loaded for 40 min with Fura-2 AM-ester (5 μM) added to the buffer solution (37°C) containing (in mM) 2 $CaCl_2$; 5.4 KCl; 0.4 MgSO4; 135 NaCl; 10 D-glucose; 10 HEPES and BSA (0.1%). Cells were washed and transferred to a chamber on the stage of a fluorescent microscope for recording (Axio Observer 7 with fast filterwheel and Digi-4 for the excitation, Zeiss). Rat Schwann cells and rat DRG

neurons were exposed to AITC (1 mM or 10 μM, respectively) or vehicle (0.5% DMSO) or CGRP (10 μM) or vehicle (0.9% NaCl), and the Ca^{2+} response was monitored for 6 min or 30 min after stimulus, respectively. The Ca^{2+} response to AITC and CGRP and was also monitored in the presence of A-967079 (50 μM), olcegepant (100 nM) or vehicle (0.1% DMSO). Some experiments were performed in a calcium-free buffer solution containing EDTA (1 mM). Rat DRG neurons were identified by challenging cells with a high (50 mM) KCl concentration that does not activate non-neuronal cells. Results were expressed as per cent increase in $Ratio_{340/380}$ over baseline normalized to the maximum effect induced by ionomycin (5 μM) added at the end of each experiment.

2.9 | RT-qPCR

Total RNA was extracted from cultured rat Schwann cells, rat DRGsand rat sciatic nerves at day 15 after CCI, pSNL and sham procedure using the RNeasy Mini Kit (Qiagen SpA, Hilden, Germany), according to the manufacturer's protocol. RNA concentration and purity were assessed spectrophotometrically by measuring the absorbance at 260 and 280 nm. The purified RNAs were reverse transcribed using SuperScript™ IV VILO™ master mix with ezDNase™ enzyme, according to the manufacturer's protocol. The KAPA SYBR® FAST universal kit was used for the amplification and the cycling conditions were as follows: samples were heated to 95°C for 10 min followed by 40 cycles of 95°C for 10 and 65°C for 20 s. PCR reaction was performed in triplicate for each sample. Relative expression of mRNA was calculated using the $2^{-\Delta(\Delta CT)}$ comparative method, with each gene normalized against the β-actin. For relative quantification of mRNA compared to housekeeping gene, real- time PCR was carried out using the Rotor Gene Q (Qiagen Spa). Sets of primers were listed as follows: ACTB-Primer1 (β-actin-Primer1): 5′-AGTACAACCTTCTTGCAGCTC-3′, ACTB-Primer2 (β-actin-Primer2): 5′-GGAGCCGTTGTCGACGA-3′ (NCBI Reference Sequence [Ref Seq]: NM_031144); TRPA1-Primer1: 5′-GCATGTACAACGAAGTGATCAAG-3′, TRPA1-Primer2: 5′-CTGTGTTCCCATTCTCTCCTT-3′ (NCBI Reference Sequence [Ref Seq]: NM_207608); AVIL-Primer1: 5′-TCTTTCTGCTTTGGACTCAGG-3′, AVIL-Primer2: 5′-GTCACCATCACAGAGAAGCTC-3′ (NCBI Reference Sequence [Ref Seq]: NM_024401): S100A1-Primer1: 5′-AGACCTGCTACAAACTGAACTC-3′, S100A1-Primer2: 5′-CTTCCCCATCTCCATTCTCATC′3′ (NCBI Reference Sequence [Ref Seq]: NM_024401: NM_001007636).

2.10 | H_2O_2 assay

H_2O_2 level was assessed in rat sciatic nerves at day 15 after CCI, pSNL, or sham procedure, or 0.5 h after CGRP, AITC and capsaicin injection (i.pl.), by using the Amplex Red® assay (Invitrogen). Briefly, tissue was rapidly removed and placed into modified Krebs/HEPES buffer (composition in mmol L^{-1}: 99.01 NaCl, 4.69 KCl, 2.50 $CaCl_2$, 1.20 $MgSO_4$, 1.03 KH_2PO_4, 25.0 $NaHCO_3$, 20.0 Na-HEPES and 5.6 glucose [pH 7.4]). Samples were minced and incubated with Amplex red (100 μM) and HRP (1 U ml^{-1}) (1 h, 37°C) in modified Krebs/HEPES buffer protected from light. Fluorescence excitation and emission were at 540 and 590 nm, respectively. H_2O_2 production was calculated using H_2O_2 standard and expressed as μmol L^{-1} mg^{-1} of dry tissue.

2.11 | Synthesis and imaging of A1CA probe

The fluorescent probe A1CA was synthesized as previously reported (Qiao et al., 2020). Briefly, 7-(diethylamino)-2-oxo-2H-chromene-3-carbonyl chloride was obtained from the reaction of 7-(diethylamino)-2-oxo-2H-chromene-3-carboxylic acid (271 mg, 1.04 mmol) with oxalyl chloride (877 μl, 10.4 mmol) in anhydrous dichloromethane (DCM, 20 ml). DMF (40 μl) was then added as catalyst. The mixture was stirred under argon atmosphere for 2 h at RT and after removal of the solvent, the desired product was used in the next step without further purification. Then, 4-[2-(4-aminophenyl) diazen-1-yl]aniline (50 mg, 0.24 mmol) was suspended in anhydrous DCM (5 ml) and triethylamine (500 μl) under argon atmosphere. A solution of 7-(diethylamino)-2-oxo-2H-chromene-3-carbonyl chloride in DCM was added dropwise and the reaction solution was kept stirring for 5 h. The solvent was then removed under vacuum and the residue was purified semi-preparative HPLC to yield a brownish solid compound (30% yield). The purity of A1CA was assessed by analytical HPLC showing a degree of purity >95%. ^1H and ^{13}C NMR characterization matches literature data. Analytical HPLC analyses were performed on a reverse-phase HPLC using a Beckman 126 liquid chromatograph equipped with a Beckman 168 UVvis detector (monitoring at 220 and 254 nm). RP-HPLC analytical gradients were run using a solvent system consisting of A (H_2O + 0.1% TFA) and B (CH_3CN + 0.1% TFA). Mass spectra were recorded with a Micromass ZMD 2000 instrument dissolving the samples in a solution of H_2O/CH_3CN/TFA (40:60:0.1). ^1H NMR and ^{13}C NMR were recorded on a Varian 400 spectrometer and were referenced to residual ^1H signals of the deuterated solvent DMSO-d_6 (δ ^1H 2.50).

HEK293T, ratTRPA1-HEK293T and primary cultured Schwann cells were incubated with A1CA (10 μM) for 3 min and washed 3 times with PBS buffer. Then the cells were placed under a Axio Observer 7 (ZEISS, Stuttgart, Germany) with 60× oil objective lens for fluorescence imaging with excitation at 405 nm and acquisition at 470–520 nm.

2.12 | Data and statistical analysis

Results are expressed as mean ± SEM. For multiple comparisons, a one-way ANOVA was used. For behavioural experiments with repeated measures, the two-way mixed model ANOVA F was used. Post hoc Bonferroni's test was conducted only if F in ANOVA achieved $P < 0.05$. Statistical analyses were performed on raw data using Graph Pad Prism 8 (GraphPad Software Inc.). P values less than 0.05

($P < 0.05$) were considered significant. Sample size for each analysis is reported in the figure legend. The data and statistical analysis comply with the recommendations of the *British Journal of Pharmacology* on experimental design and analysis in pharmacology (Curtis et al., 2022).

2.13 | Materials

If not otherwise indicated, reagents were obtained from Merck Life Science SRL (Milan, Italy). Details of other materials and suppliers were provided in the specific sections

2.14 | Nomenclature of targets and ligands

Key protein targets and ligands in this article are hyperlinked to corresponding entries in the IUPHAR/BPS Guide to PHARMACOLOGY http://www.guidetopharmacology.org and are permanently archived in the Concise Guide to PHARMACOLOGY 2021/22 (Alexander et al., 2021).

3 | RESULTS

3.1 | AITC and capsaicin-evoked nocifensive behaviour and mechanical allodynia

If not otherwise specified, all compounds were given by the intraplantar (i.pl., 20 µl) route of administration. Injection of AITC (200 nmol) in the hind paw of Sprague–Dawley rats caused a spontaneous, acute and transient (~10 min) local nocifensive behaviour that was followed by a delayed and prolonged (~2 h) hind paw mechanical allodynia (HPMA) (Figure 1a). Systemic (i.p. 100 mg kg^{-1}) or local (i.pl., 300 nmol) pretreatment with the selective TRPA1 antagonist, A-967079, prevented both nocifensive behaviour and HPMA induced by AITC (Figure 1a). Selective involvement of the TRPA1 channel was strengthened by the failure of the TRPV1 antagonist capsazepine to affect either response (Figure S1). Capsaicin (10 nmol) injection elicited a similar biphasic response, consisting of an acute nocifensive behaviour (~10 min) and a delayed HPMA (~2 h), which were abated by pretreatment (i.p., 4 mg kg^{-1}) with the selective TRPV1 antagonist, capsazepine (Figure 1b). Notably, pretreatment

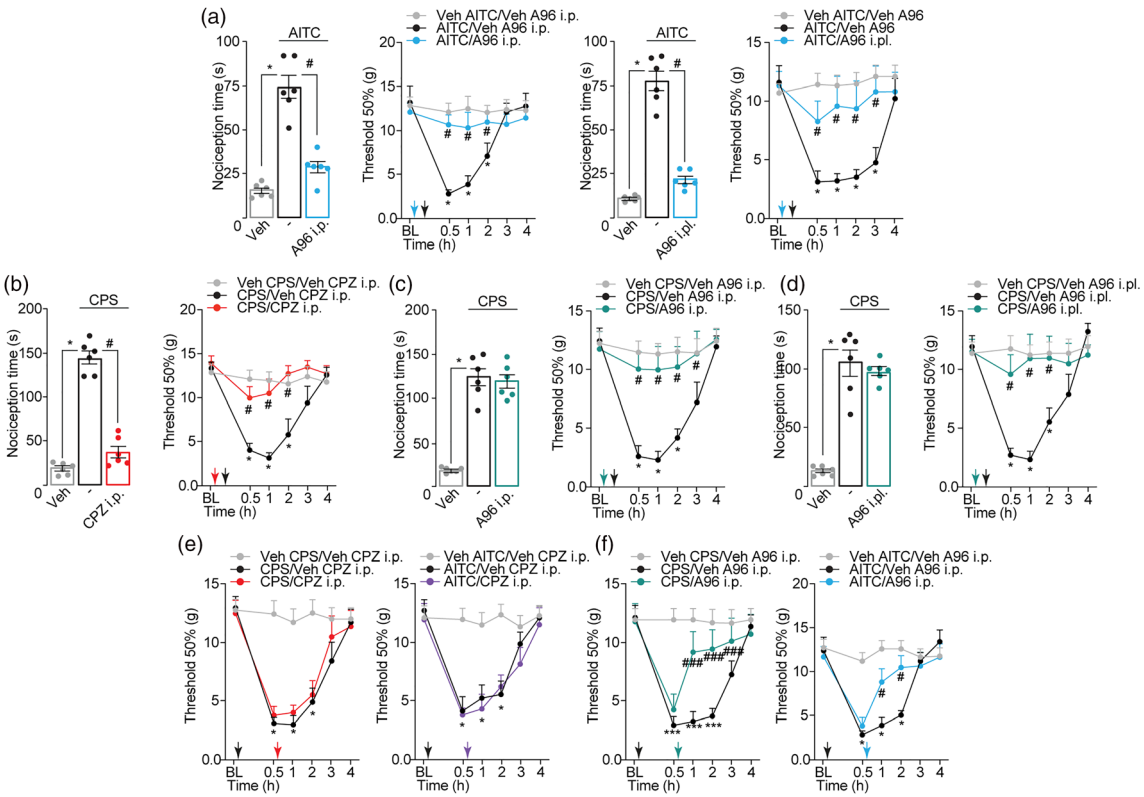

FIGURE 1 AITC and capsaicin-evoked nocifensive behaviour and mechanical allodynia. (a) Acute nocifensive behaviour and hind paw mechanical allodynia (HPMA) after intraplantar (i.pl., 20 µl), AITC (200 nmol) or vehicle (veh) in rats pretreated (0.5 h) with intraperitoneal (i.p.) or local (i.pl.) A-967079 (A96, 100 mg kg^{-1} and 300 nmol, respectively) or veh. (b) Acute nocifensive behaviour and HPMA after capsaicin (CPS, 10 nmol, i.pl.) or veh in rats pretreated (0.5 h) with capsazepine (CPZ, 4 mg kg^{-1}, i.p.) or veh. (c) Acute nocifensive behaviour and HPMA after CPS (10 nmol, i.pl.) or veh in rats pretreated (0.5 h) with A96 (100 mg kg^{-1}, i.p.) and A96 (300 nmol, i.pl.) or veh. (d) HPMA after CPS (10 nmol, i.pl.), AITC (200 nmol, i.pl.) or veh in rats post-treated (0.5 h) with CPZ (4 mg kg^{-1}, i.p.), A96 (100 mg kg^{-1}, i.p.) or veh. Mean ± SEM, n = 6 rats per group. Dash (-) is a combination of vehicles. Arrows indicates time of administration. $^{*}P < 0.05$ vs. veh; $^{\#}P < 0.05$ vs. AITC/veh A96, CPS/veh CPZ, CPS/veh A96. One-way and two-way ANOVA, Bonferroni correction

with A-967079 (i.p. or i.pl.) did not affect the nocifensive behaviour but did prevent HPMA induced by capsaicin (Figure 1c,d).

To understand the mechanism underlying TRPA1-dependent HPMA, antagonists were given after the administration of the stimulus. Post-treatment with capsazepine did not affect HPMA elicited by both capsaicin and AITC (Figure 1e), whereas post-treatment with A-967079 markedly attenuated both responses (Figure 1f). These data suggest that spontaneous nocifensor behaviour elicited by TRPV1 and TRPA1 activators are mediated by the activation of the respective channel in the sensory nerve terminal. However, whatever the initial stimulus targeting the peptidergic nerve terminal, the prolonged HPMA is due to a common pathway implicating the TRPA1 channel.

3.2 | SP and CGRP-evoked mechanical allodynia

Based on the notion that, in rodents, both capsaicin and AITC release the proinflammatory neuropeptides, CGRP and SP (Geppetti & Holzer, 1996), and on previous findings obtained in mice (De Logu et al., 2022), we hypothesized that a neurogenic inflammatory mechanism is implicated in HPMA evoked by capsaicin or AITC. Pretreatment with an antagonist of the **NK_1 receptor**, L733,060 (20 nmol), attenuated HPMA evoked by SP (3.5 nmol) (Figure 2a) and pretreatment with the CGRP receptor antagonist, olcegepant (1 nmol), reduced HPMA elicited by CGRP (1.5 nmol) (Figure 2b). No spontaneous acute nocifensive behaviour was observed following injection of either SP or CGRP (Figure 2a,b).

Neither olcegepant nor L733,060 inhibited the nocifensor behaviour evoked by AITC or capsaicin (Figure 2c–f). However, whereas pretreatment with L733,060 was ineffective (Figure 2e,f), pretreatment with olcegepant prevented HPMA elicited by both AITC and capsaicin (Figure 2c,d). Notably, both pretreatment and post-treatment with A-967079 (300 nmol) attenuated HPMA evoked CGRP (Figure 2g,h). In contrast, pretreatment with capsazepine (i.p., 4 mg kg^{-1}) (Figure 2i) or post-treatment with olcegepant (1 nmol) (Figure 2j) failed to reduce HPMA evoked by CGRP. In addition, post-treatment with olcegepant did not affect HPMA elicited by either AITC (Figure 2k) or capsaicin (Figure 2l). These data indicate that, in

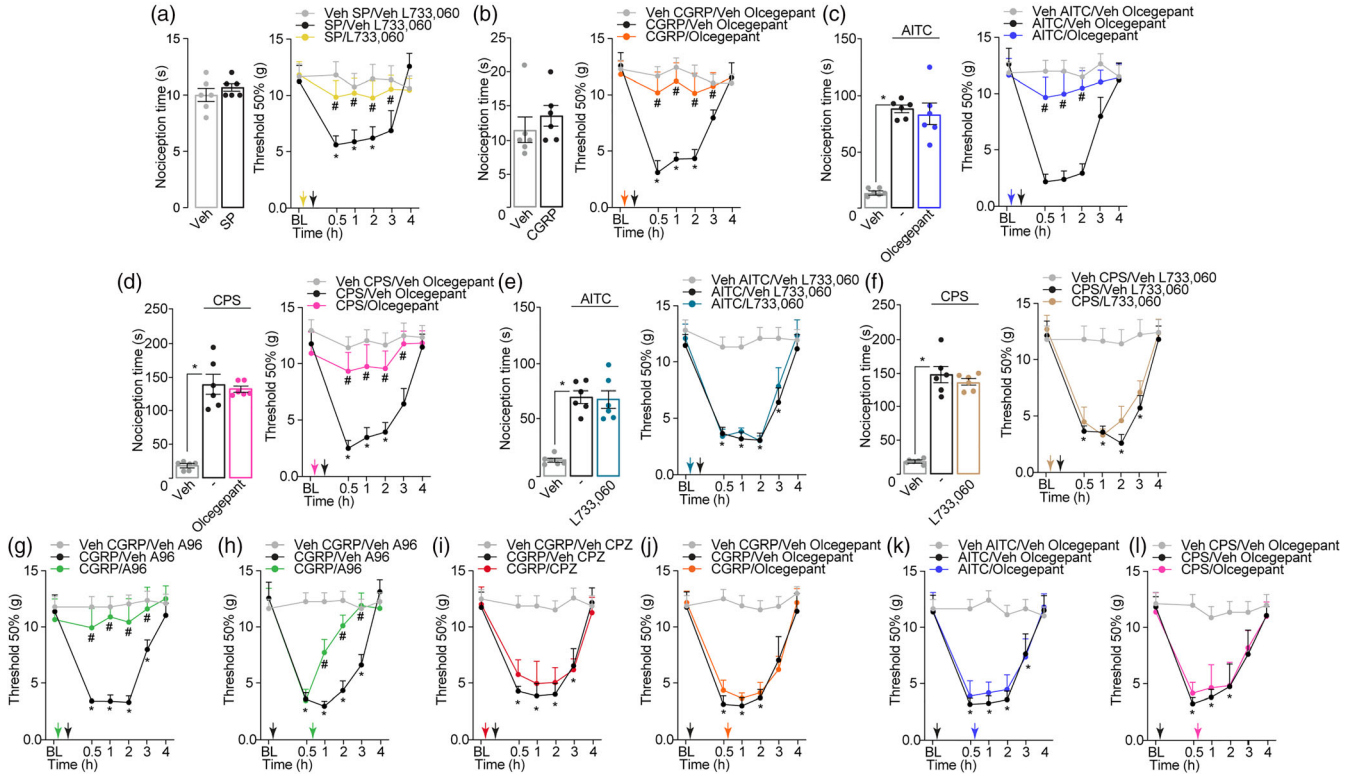

FIGURE 2 SP and CGRP-evoked mechanical allodynia. (a) Acute nocifensive behaviour and hind paw mechanical allodynia (HPMA) after intraplantar (i.pl., 20 µl), SP (3.5 nmol) or vehicle (veh) in rats pretreated (0.5 h) with local (i.pl.) L733,060 (20 nmol) or veh. (b) Acute nocifensive behaviour and HPMA after CGRP (1.5 nmol, i.pl.) or veh in rats pretreated (0.5 h) with olcegepant (1 nmol) or veh. Acute nocifensive behaviour and HPMA after AITC (c) (200 nmol, i.pl.), capsaicin (d) (CPS, 10 noml, i.pl.) or veh in rats pretreated (0.5 h) with olcegepant (1 nmol) or veh. Acute nocifensive behaviour and HPMA after AITC (e) (200 nmol, i.pl.), capsaicin (f) (CPS, 10 noml, i.pl.) or veh in rats pretreated (0.5 h) with L733,060 (20 nmol) or veh. HPMA after CGRP (1.5 nmol, i.pl.) or veh in rats pretreated (g) (0.5 h) or post-treated (h) (0.5 h) with A-967079 (A96, 300 nmol, i.pl.) or veh. HPMA after CGRP (1.5 nmol, i.pl.) or veh in rats pretreated (0.5 h) with capsazepine (i) (CPZ, 4 mg kg^{-1}, intraperitoneal, i.p.) or veh, or (k) in rats post-treated (0.5 h) with olcegepant (1 nmol) or veh. Mean ± SEM, n = 6 rats per group. Dash (-) is a combination of vehicles. Arrows indicates time of administration. $^{*}P < 0.05$ vs. veh; $^{\#}P < 0.05$, $^{\#\#\#}P < 0.001$ vs. SP/veh L733,060, CGRP/veh olcegepant, CPS/veh olcegepant, CGRP/veh A96. One-way and two-way ANOVA, Bonferroni correction

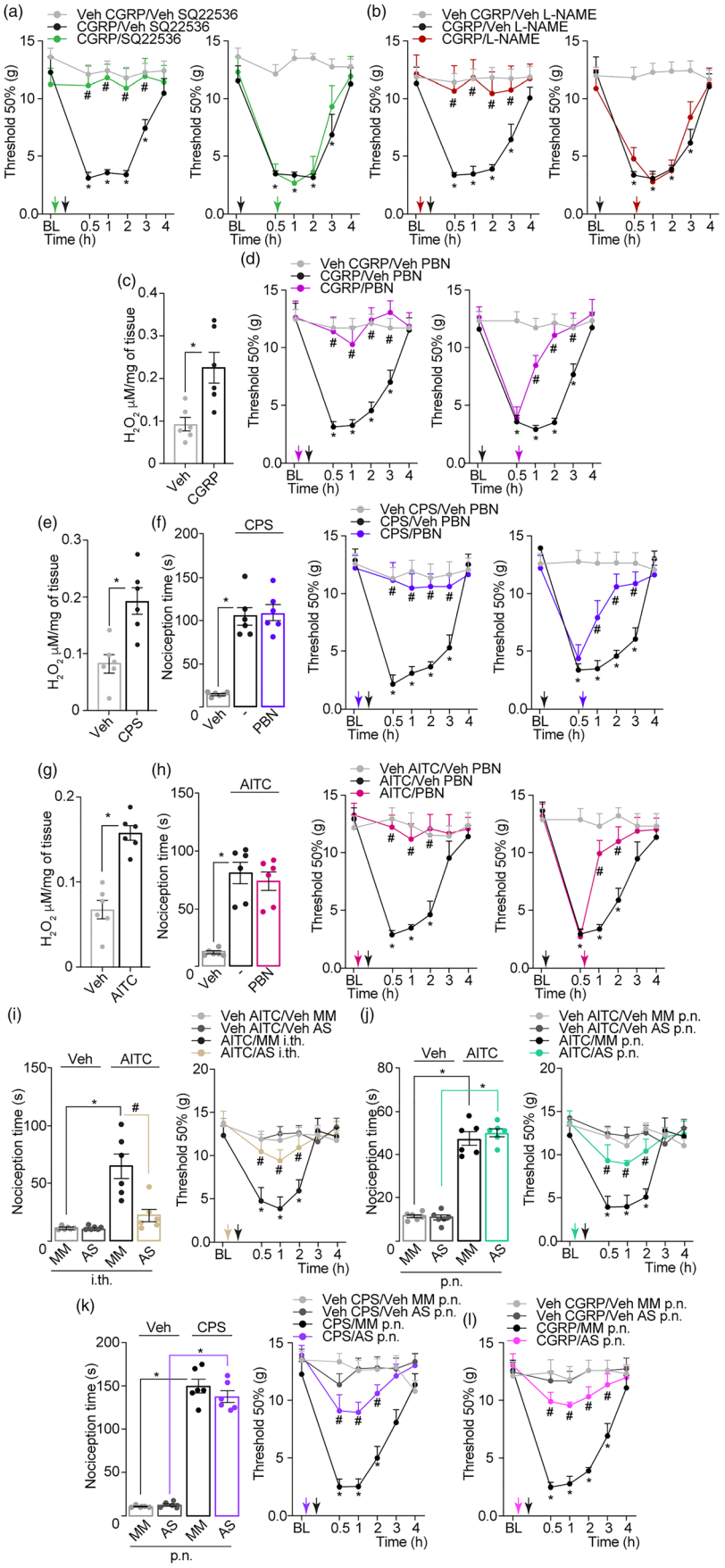

FIGURE 3 Legend on next page.

rats, HPMA associated with neurogenic inflammation is due to CGRP released from TRPV1/TRPA1 expressing nerve terminals and, while TRPV1 activation and CGRP release have an initial role, solely TRPA1 sustains the 2–3 h of HPMA.

3.3 | Cellular and molecular mediators of neurogenic inflammation associated allodynia

Having established the critical role of CGRP in capsaicin- and AITC-induced HPMA and based on mouse findings (De Logu et al., 2022), we explored the signalling pathway underlying CGRP-induced HPMA. Pretreatment, but not post-treatment, with the **adenylyl cyclase** inhibitor, SQ22536 (25 nmol), or the **nitric oxide synthase (NOS)** inhibitor, **L-NG-nitro arginine methyl ester (L-NAME**, 1 μmol), prevented CGRP-evoked HPMA (Figure 3a,b). CGRP, capsaicin and AITC (i.pl.) increased the content of a ROS marker, **H_2O_2**, in the sciatic nerve tissue (Figure 3c,e,g). Both pretreatment and post-treatment with the ROS scavenger, N-tert-butyl-alpha-phenylnitrone (PBN, 670 nmol), inhibited HPMA evoked by CGRP (Figure 3d), capsaicin (Figure 3f), or AITC (Figure 3h). However, PBN did not affect acute nocifensor behaviour evoked by capsaicin or AITC (Figure 3f,h). Thus, HPMA induced by CGRP capsaicin or AITC in rats shares a final common pathway that encompasses an early and transient activation of adenylyl cyclase and NOS and a sustained generation of ROS.

To investigate the role of extraneuronal TRPA1 expressed in local cells of the rat paw in neurogenic inflammation-dependent HPMA, a TRPA1 antisense oligonucleotide (AS-ODN), or the mismatched oligonucleotide (MM-ODN), were injected perineurally (p.n., 10 nmol) to silence TRPA1 in local perineural cells or intrathecally (i.th., 10 nmol) to silence TRPA1 in nociceptors (Bonet et al., 2013). Injection (i.th.) of TRPA1 AS-oligonucleotide eliminated both the acute nocifensor behaviour and HPMA to AITC (Figure 3f). In contrast, (p.n.) TRPA1 AS-oligonucleotide, which does not interfere with neuronal RNA, did not affect acute nocifensor behaviour, but attenuated HPMA evoked by AITC (Figure 3g). Treatment (p.n.) with TRPA1 AS-oligonucleotide did not affect acute nocifensor behaviour evoked by capsaicin, but reduced HPMA elicited by either capsaicin or CGRP (Figure 3h,i).

The expression of TRPA1 mRNA in rat Schwann cells was confirmed by RNAscope in rat sciatic nerve tissue and primary culture of rat Schwann cells by co-expression of TRPA1 mRNA with staining for the Schwann cell marker, S100 (Figure 4a,b). Primary rat Schwann cells were harvested and grown in culture and their identity was verified by RT-qPCR with the S100 gene expression (Figure 4c). TRPA1 mRNA expression was also confirmed in cultured rat Schwann cells and DRG neurons (Figure 4c). The identity of DRG neurons was verified by advillin (AVIL) gene expression (Figure 4c).

Exposure of cultured primary rat Schwann cells and DRG neurons to AITC elicited a rapidly developing calcium response (Figure 4d,e) that was inhibited in the presence of A-967079 and in calcium-free medium. Exposure to CGRP elicited a delayed calcium response in rat Schwann cells (but not in DRG neurons) that was attenuated by olcegepant, A-967079 and calcium-free medium (Figure 4f,g). The delayed response to CGRP confirms previous results observed in human Schwann cells that the activation of a series of intracellular mediators is required to elicit a TRPA1-dependent calcium response (De Logu et al., 2022). Activation of the rat Schwann cell CT receptor/**RAMP1** by CGRP increased cAMP and induced a **PKA**-dependent activation of **endothelial NOS (eNOS)** and the resulting increase in **NO** eventually targeted TRPA1.

To further verify the TRPA1 protein expression in rat Schwann cells, a photochromic selective TRPA1 ligand (A1CA) was used (Qiao et al., 2020). A1CA exhibits no fluorescence in free style due to the free rotation of rotors. However, its interaction with TRPA1 inhibits the rotation and enhances the fluorescence (Qiao et al., 2020). rTRPA1-HEK293T transfected cells, HEK293T cells and cultured primary rat Schwann cells were exposed to A1CA (10 μM) for three minutes and then visualized with a fluorescent microscope. rTRPA1-HEK293T cells and cultured primary rat Schwann cells, but not HEK293T cells, showed fluorescence, indicating A1CA and TRPA1 interaction that restricts molecular rotation (Figure 4h).

3.4 | TRPA1 role in chronic constriction injury (CCI) and partial sciatic nerve ligation (pSNL)

Rats undergoing CCI or pSNL developed, at day 15 after surgery, a robust HPMA ipsilateral to the lesion that was not observed in sham rats. Systemic (i.p.) administration of two different TRPA1 antagonists, AMG-0902 and A-967079, while not affecting HPMA

FIGURE 3 CGRP, AITC and capsaicin induce mechanical allodynia via NO and ROS production. Hind paw mechanical allodynia (HPMA) after intraplantar (i.pl., 20 μl) CGRP (1.5 nmol) or vehicle (veh) in rats pretreated (0.5 h) or post-treated (0.5 h) with local (i.pl.) (a) SQ22536 (25 nmol), (b) L-NAME (1 μmol) or veh. (c) H_2O_2 levels in the sciatic nerve of rat after CGRP (1.5 nmol, i.pl.) or veh. (d) HPMA after CGRP (1.5 nmol, i.pl.) or veh in rats pretreated (0.5 h) or post-treated (0.5 h) with local (i.pl.) PBN (670 nmol) or veh. (e,g) H_2O_2 levels in the sciatic nerve of rat after capsaicin (CPS, 10 nmol, i.pl.), AITC (200 nmol, i.pl.) or veh. Acute nocifensive behaviour and HPMA after (f) capsaicin (CPS, 10 nmol, i.pl.), (h) AITC (200 nmol, i.pl.) or veh in rats pretreated (0.5 h) or post-treated (0.5 h) with local (i.pl.) PBN (670 nmol) or veh. Acute nocifensive behaviour and HPMA after AITC (200 nmol, i.pl.) or veh in rats treated (once a day for four consecutive days) with (i) intratechal (i.th, 10 μl) or (J) perineural (p.n., 10 μl) TRPA1 antisense (AS) or mismatch (MM) oligonucleotide (ODN) (10 nmol). Acute nocifensive behaviour and HPMA after (k) CPS (10 nmol, i.pl.), (l) CGRP (1.5 nmol, i.pl.) or veh in rats treated (once a day for four consecutive days) TRPA1 AS/MM ODN (10 nmol). Mean ± SEM, n = 6 rats per group. Arrows indicates time of administration. $^*P < 0.05$ vs. veh; $^{\#}P < 0.05$ vs. CGRP/veh SQ22536, L-NAME, PBN, CPS-AITC/veh PBN, AITC-CPS-CGRP/MM. One-way and two-way ANOVA, Bonferroni correction

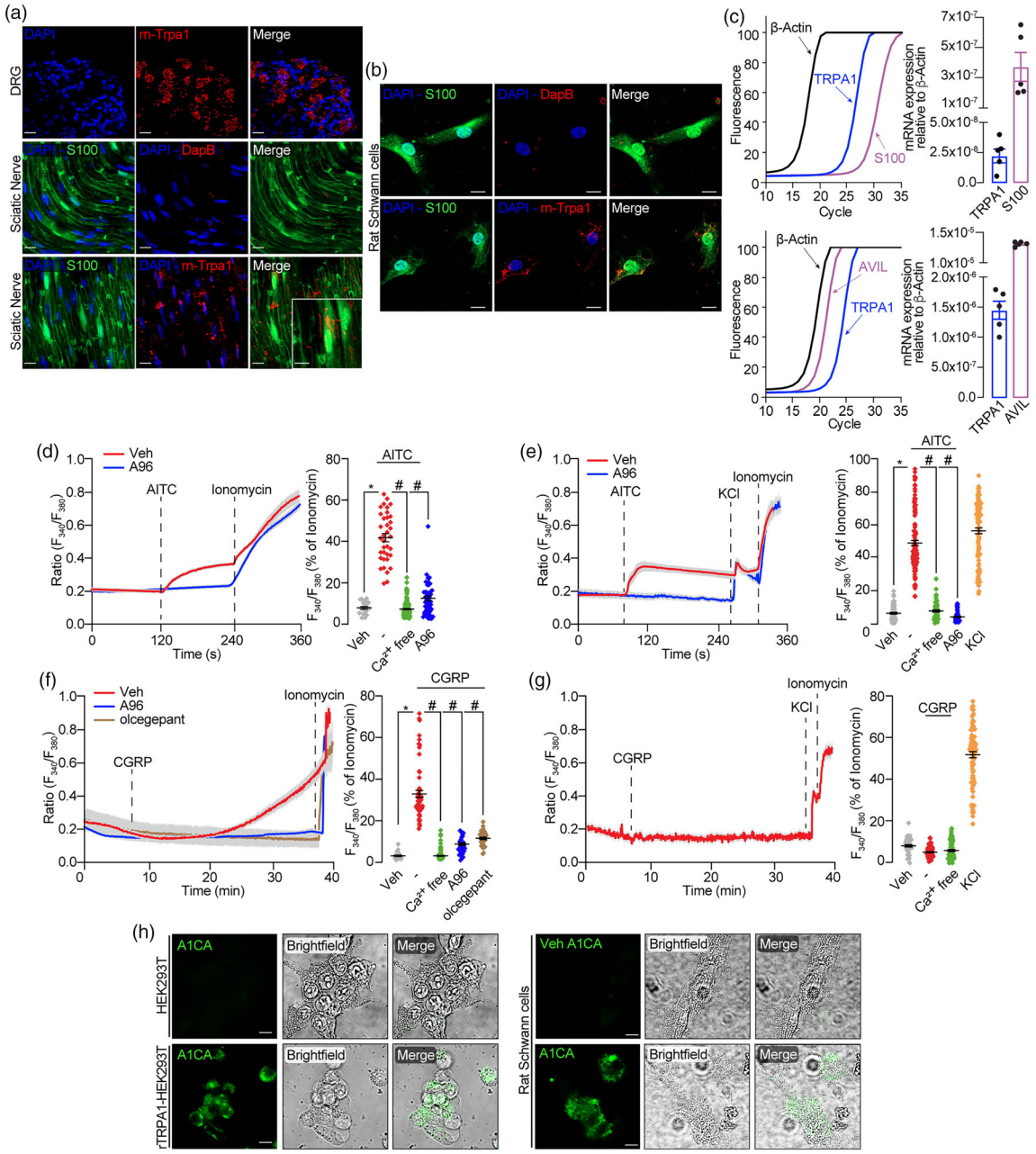

FIGURE 4 TRPA1 expression and function in primary rat Schwann cells. (a) Representative images of TRPA1 mRNA expression in rat dorsal root ganglia (DRGs) and sciatic nerve (scale bar: 20 μm, inset 10 μm) (n = 5 subjects) and (b) primary rat Schwann cells (scale bar: 5 μm) (n = 5 independent experiments). DapB, negative control. (c) Representative real-time PCR plot and cumulative data for S100 and Trpa1 mRNA in cultured primary rat Schwann cells and for AVIL and Trpa1 DRG neurons (n = 5 independent experiments). (d,e) Typical traces and cumulative data of calcium (Ca^{2+}) response (F_{340}/F_{380}) in primary rat Schwann cells and DRG neurons stimulated with AITC (1 mM or 10 μM, respectively) or vehicle (veh) in presence of A-967079 (A96, 50 μM), veh or in a Ca^{2+}-free medium (rat Schwann cells number: AITC = 36, veh = 20, A96 = 46 and Ca^{2+}-free = 149, n = 5 independent experiments; DRG neurons number: AITC = 132, veh = 69, A96 = 80 and Ca^{2+}free = 73, n = 5 independent experiments). (f,g) Typical traces and cumulative data of Ca^{2+} response (F_{340}/F_{380}) in primary rat Schwann cells and DRG neurons stimulated with CGRP (10 μM) or vehicle (veh) in presence of olcegepant (100 nM) or A-967079 (A96, 50 μM), veh or in a Ca^{2+}-free medium (rat Schwann cells number: CGRP = 62, veh = 27,olcegepant = 34, A96 = 34,and Ca^{2+}-free = 132, n = 5 independent experiments; DRG neurons number: CGRP = 102, veh = 44 and Ca^{2+}-free = 79, n = 5 independent experiments). (h) Fluorescence and bright field images of probe A1CA (10 μM) in HEK293T cells, rTRPA1-HEK293T transfected cells and primary cultured rat Schwann cells (scale bar: 5 μm). Mean ± SEM. Dash (-) is a combination of vehicles. *$P < 0.05$ vs. veh; #$P < 0.05$ vs. AITC CGRP. One-way ANOVA, Bonferroni correction

associated with CCI (Figure 5a), dose-dependently attenuated HPMA associated with pSNL (Figure 5b). Capsazepine (i.p.) failed to reduce HPMA in either the CCI or the pSNL model (Figure 5c,d). Repeated (from day 10 to day 14) injection (p.n.) of the TRPA1 AS-oligonucleotide did not affect HPMA in the CCI model, whereas it reduced HPMA in the pSNL model (Figure 5e,f). TRPA1 mRNA expression in sciatic nerve tissue was not affected by CCI or pSNL compared to sham procedure (Figure 5g). The role of CGRP in both models was also explored. At day 15 after surgery, olcegepant (1 nmol) failed to reduce HPMA in either the pSNL or the CCI model (Figure 5h,i). Finally, the role of oxidative stress was tested in both models. CCI and pSNL increased H_2O_2 levels in sciatic nerve tissue at day 15 after surgery (Figure 5j,l). Of note, inhibition of HPMA by N-tert-butyl-α-phenylnitrone was superior in pSNL (AUC, 42.56 ± 1.73 n = 6) than in the CCI (AUC, 33.20 ± 3.03 n = 6, $P < 0.05$) model (Figure 5k,m).

4 | DISCUSSION

A large series of evidence supports the role of TRPA1 in models of inflammatory, neuropathic, cancer and migraine pain in mice (De Logu et al., 2021, 2022, 2017; Trevisan et al., 2014). However, recent findings obtained in rats with genetic deletion of the TRPA1 channel by the CRISPR technology showed that, while the agonist-induced TRPA1-mediated acute nocifensor behaviour was attenuated, mechanical allodynia produced by neuropathic and inflammatory pain models was unaffected (Reese et al., 2020). From these findings, the hypothesis was advanced that the pro-algesic role of TRPA1 is confined to mice and it cannot be replicated in another rodent species and possibly in other species (Reese et al., 2020). Here, based on recent findings obtained in mice (De Logu et al., 2022), we explored in rats the role of TRPA1 in mechanical allodynia associated with neurogenic inflammation or neuropathic pain models.

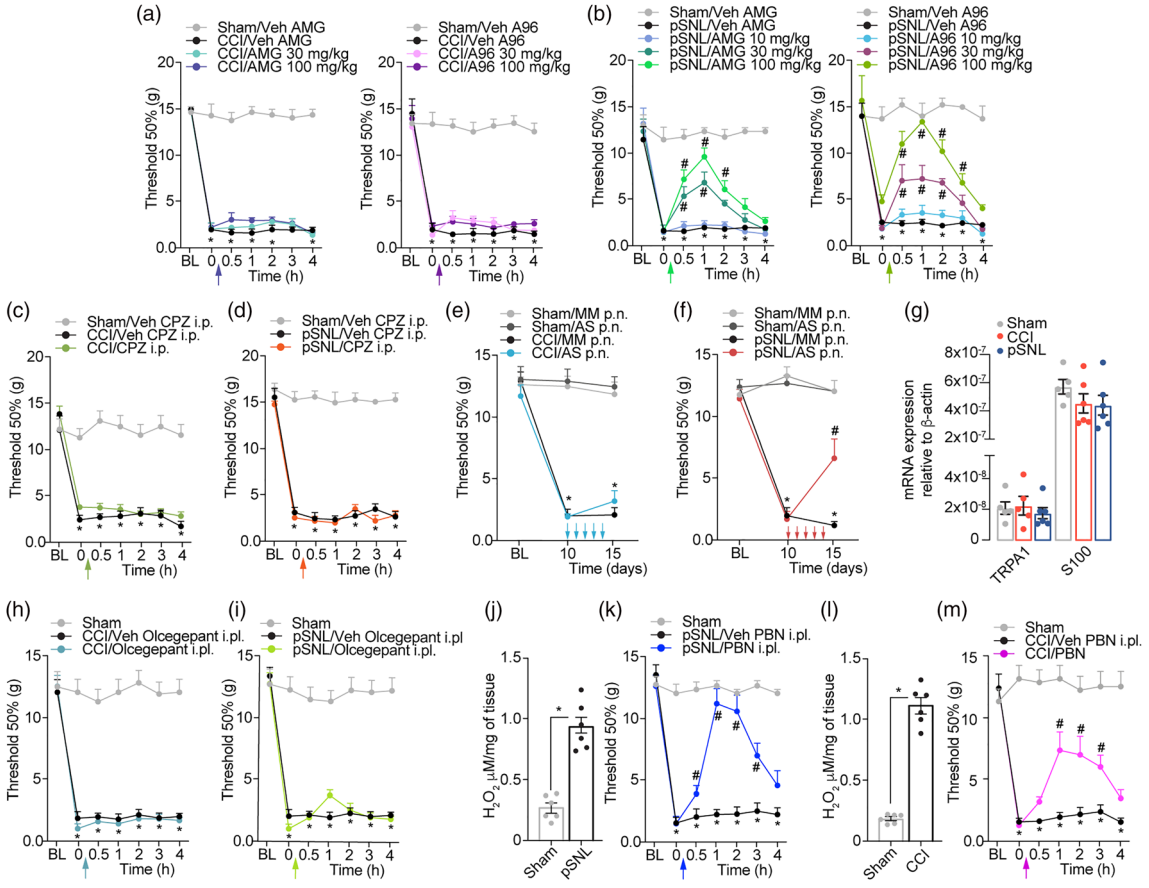

FIGURE 5 TRPA1 activation mediates hind paw mechanical allodynia (HPMA) in partial sciatic nerve ligation (pSNL), but not in chronic constriction injury (CCI) model. HPMA in rats 15 days after (a) CCI, (b) pSNL or sham procedure treated with intraperitoneal (i.p.) AMG0902 (AMG, 30 and 100 mg kg^{-1}), A-967079 (A96, 10, 30 and 100 mg kg^{-1}) or vehicle (veh). HPMA in rats 15 days after (c) CCI, (d) pSNL or sham procedure treated with capsazepine (CPZ, 4 mg kg^{-1}, i.p.) or veh. HPMA in rats 15 days after (e) CCI, (f) pSNL or sham procedure treated (once a day for four consecutive days starting from day 10 to day 14 after surgery) with perineural (p.n., 10 μl) TRPA1 antisense (AS) or mismatch (MM) oligonucleotide (ODN) (10 nmol). (g) Cumulative data for Trpa1 and S100 mRNA in rat sciatic nerve tissue 15 days after pSNL, CCI or sham procedure (n = 6 rats per group). HPMA in rats 15 days after (h) CCI, (i) pSNL or sham procedure treated with intraplantar (i.pl.) olcegepant (1 nmol) or veh. HPMA in rats 15 days after (i) CCI, (j) pSNL or sham procedure treated with N-tert-butyl-α-phenylnitrone (PBN; 670 nmol, i.pl.) or veh. Mean ± SEM, n = 6 rats per group. Arrows indicate time of administration. *$P < 0.05$ vs. sham/veh; #$P < 0.05$ vs. pSNL-CCI/veh AMG/A96, pSNL/MM, pSNL-CCI/veh PBN. Two-way ANOVA, Bonferroni correction

We report that selective activation of TRPV1 and TRPA1 in the rat hind paw elicited acute and transient nocifensor behaviours that were most likely due to the direct TRPV1 or TRPA1 gating by the respective activators and the ensuing depolarization that conveys pain signals to the central nervous system. The transient nature of the nocifensor responses could be associated to the limited time of channel occupancy by the activators. About 30 min after the injection, rats developed a delayed and sustained mechanical allodynia that lasted 2–3 h. A similar acute and transient nocifensor behaviour followed by a delayed and sustained periorbital mechanical allodynia (PMA) has been observed in mice after the periorbital injection of capsaicin (De Logu et al., 2022). The underlying mechanism of the capsaicin-evoked hind paw mechanical allodynia (HPMA) in rats and periorbital mechanical allodynia in mice is apparently identical.

In rats and mice, pretreatment with a CGRP receptor antagonist, but not with a NK_1 receptor antagonist, prevented capsaicin-evoked HPMA and PMA, respectively. These previous (De Logu et al., 2022) and present findings indicate that one (CGRP) of the two neuropeptide mediators of neurogenic inflammation elicits HPMA. Thus, the association of HPMA with neurogenic inflammation appears to be robustly proven here and previously (De Logu et al., 2022) by the observation that capsaicin-evoked CGRP release, which mediates the vasodilatatory component of neurogenic inflammation (Russell et al., 2014; Sinclair et al., 2010), also mediates HPMA. The sequence of intracellular mediators that in mice (De Logu et al., 2022) promotes the pro-algesic action of CGRP was replicated in rats, as adenylyl cyclase and NOS inhibitors, a ROS scavenger and a TRPA1 antagonist, attenuated CGRP- and capsaicin-evoked HPMA. However, whereas CGRP receptor antagonist, and adenylyl cyclase and NOS inhibitors prevented HPMA if drugs were given before, but not after the stimulus, both pretreatment and post-treatment with a ROS scavenger or a TRPA1 antagonist were equally effective in reducing HPMA. The interpretation of these findings suggests that CGRP, cyclic AMP and NO exert an early and transient role in HPMA associated with neurogenic inflammation, whereas ROS, which directly activate TRPA1 (Bessac et al., 2008), promote a feed-forward pathway that sustains mechanical allodynia over 2–3 h. As AITC-evoked HPMA was attenuated by the same pharmacological interventions and with the same timing that were shown to inhibit capsaicin-evoked HPMA, an identical common pathway is proposed to sustain mechanical allodynia associated with neurogenic inflammation, independently from the stimulus that triggers the activation of peptidergic nociceptors and the ensuing neuropeptide release (Figure 6).

In mice, we were able to identify the Schwann cells surrounding peptidergic nerve terminals as the cell type that expresses the TRPA1 that sustains the CGRP-mediated and capsaicin-evoked PMA (De Logu et al., 2022). The aim of the present study did not have this purpose and, accordingly, specific tools to selectively silence Schwann cell TRPA1 in rats were not developed. Notwithstanding, a series of findings suggests the implication of peripheral glial cells. First, in rats, RNAscope showed the colocalization of TRPA1 mRNA with immunofluorescence for the Schwann cell specific protein, S100. Second, AITC evoked a calcium response in primary cultures of rat Schwann cells that was attenuated by a TRPA1 antagonist. Third and importantly, rat Schwann cells, like mouse and human Schwann cells (De Logu et al., 2022), responded to CGRP with a delayed and sustained calcium response that was reduced by a CGRP receptor antagonist and a TRPA1 antagonist. These *in vitro* findings were repeated by *in vivo* results, as HPMA was attenuated by inhibitors of the CGRP receptor and TRPA1.

Regarding the two neuropathic pain models investigated in the present study, we confirmed (Reese et al., 2020) that, in the more severe model (CCI), HPMA was not reduced by two different TRPA1 antagonists. However, in the less severe model (pSNL), HPMA was

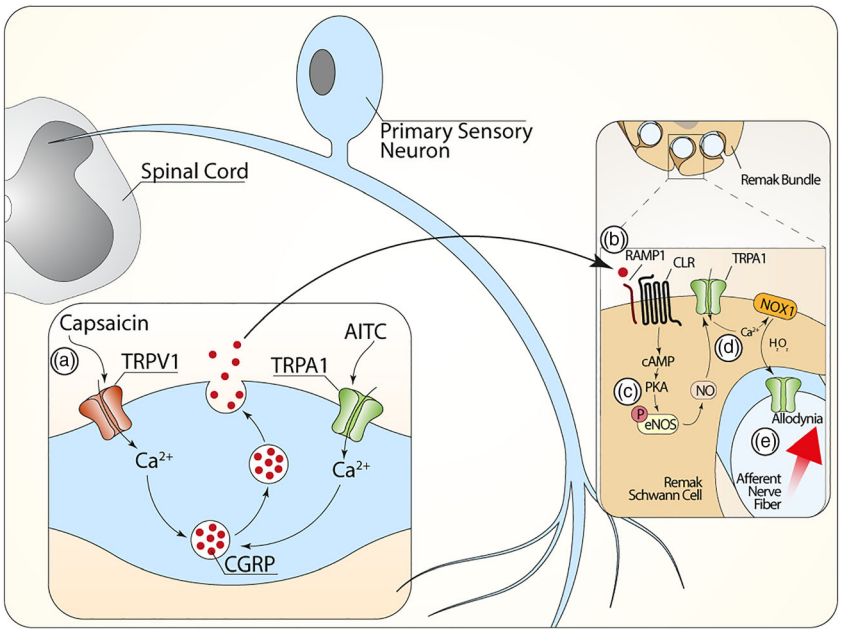

FIGURE 6 Schematic representation of the pathway that signals mechanical allodynia associated with neurogenic inflammation. In rats, (a) the selective TRPV1 and TRPA1 agonists (capsaicin and AITC, respectively) release CGRP from terminals of primary sensory neurons. (b) CGRP activates its receptor (CLR/RAMP1) on the surrounding Schwann cell. (c) CLR/RAMP1 activation promotes the formation of a series of intracellular mediators that, by the eNOS-dependent release of NO (d), eventually targets Schwann cell TRPA1. TRPA1 via **NOX1** activation release H_2O_2 that (e) targets neuronal TRPA1 to signal allodynia.

attenuated in a dose-dependent manner by the two TRPA1 antagonists. However, in the two neuropathic pain models, CGRP release does not apparently play any role as HPMA was unaffected by olcegepant. It is known that neuropathic pain caused by peripheral nerve lesion (Wallerian degeneration) is due to haematogenic macrophage accumulation at the site of the injury (De Logu et al., 2017; Van Steenwinckel et al., 2015). Oxidative stress generated by invading macrophages mediates mechanical allodynia in both models, although its contribution seems higher in the pSNL model, as the ROS scavenger, N-tert-butyl-α-phenylnitrone, appeared superior in reducing HPMA in the pSNL model than in the CCI model. The unique redox-sensitivity of TRPA1 (Hinman et al., 2006; Macpherson et al., 2007) and the higher oxidative burden in the pSNL might be the reason for the channel involvement in this model. Additional explanations may be proposed. There is evidence of remarkable differences in the nerve lesions in the footpad skin produced in rats by CCI and pSNL (Ma & Bisby, 2000). Whereas in CCI PGP-9.5+ve, nerve fibres dramatically decreased within two weeks, in the pSNL model the decrease was partial and underwent a time-dependent recovery (Ma & Bisby, 2000). It is possible to hypothesize that the less severe pSNL lesion preserves the integrity of the unit composed by the nerve fibre and the surrounding Schwann cells that contribute to mechanical allodynia. In the more severe CCI lesion, the structural loss of peripheral sensory axons excludes their contribution to generating pain signals.

A TRPA1 antagonist failed to reduce pain symptoms in patients with chronic painful diabetic neuropathy (Jain et al., 2022). However, it did produce a statistically significant attenuation in a subgroup of patients with preserved sensory nerve function and therefore with a less severe neuropathy (Jain et al., 2022). These findings show some similarity with the present rat data, where HPMA associated with a less severe nerve lesion was TRPA1-dependent. The lack of effect of a CGRP antagonist in either the CCI or pSNL model underlines the unique role of CGRP in migraine (Edvinsson et al., 2018; Nassini et al., 2014) and not in other pain conditions, as indicated by the failure of an anti-CGRP monoclonal antibody in reducing pain in patients with osteoarthrosis (Jin et al., 2018). It is possible that in Wallerian degeneration the oxidative burden required for targeting Schwann cell TRPA1 is provided by the massive ROS generation produced by invading macrophages, while under these circumstances the contribution of CGRP to the overall oxidative burden is negligible.

Primary hyperalgesia, a pain response due to sensitization of peripheral nociceptors, has been reported in the cutaneous area of inflammation following the application of a variety of stimuli, including capsaicin (LaMotte et al., 1992). The proposal by Sir Thomas Lewis (Lewis, 1936) that a chemical substance, released from collateral branches by the antidromic invasion of propagated action potentials originating from the injured nerve terminal, causes the flare (inflammation) and increases the sensitivity of other fibres responsible for pain can be applied to the present findings in rats. This mechanism, recently reported in mice (De Logu et al., 2022) and confirmed here in rats, might be a common feature that should be explored also in humans. In conclusion, we have reported that the contribution of TRPA1 to mechanical allodynia appears to be present in models of neurogenic inflammation and models of neuropathic pain characterized by moderate nerve injury, although in this latter case the contribution of CGRP is absent.

ACKNOWLEDGEMENTS

This work is supported by grants from the European Research Council (ERC) under the European Union's Horizon 2020 research and innovation programme (H2020 European Research Council) (grant agreement No. 835286) (PG).

CONFLICTS OF INTEREST

FDL, PG and RN are the founding scientists of FloNext Srl. PG has been in advisory boards and/or received fees for lectures from Novartis, Amgen, TEVA, AbbVie, Eli-Lilly and Lundbeck. The other authors have no conflicts of interest to declare.

AUTHOR CONTRIBUTIONS

FDL, PG, and RN conceived the project, analyzed the data, and wrote the manuscript; GDS, LL, MM, DSMdA, MT, AR, MC, and LFI performed the experiments and analyzed the data; VA and DP performed the synthesis and characterization of the A1CA probe.

DECLARATION OF TRANSPARENCY AND SCIENTIFIC RIGOUR

This Declaration acknowledges that this paper adheres to the principles for transparent reporting and scientific rigour of preclinical research as stated in the *BJP* guidelines for Design and Analysis, Immunoblotting and Immunochemistry and Animal Experimentation, and as recommended by funding agencies, publishers and other organizations engaged with supporting research.

DATA AVAILABILITY STATEMENT

The data that support the findings of this study are available from the corresponding author upon reasonable request.

ORCID

Francesco De Logu https://orcid.org/0000-0001-8360-6929
Antonia Romitelli https://orcid.org/0000-0003-2495-8769
Pierangelo Geppetti https://orcid.org/0000-0003-3797-8371
Romina Nassini https://orcid.org/0000-0002-9223-8395

REFERENCES

Alexander, S. P., Mathie, A., Peters, J. A., Veale, E. L., Striessnig, J., Kelly, E., Armstrong, J. F., Faccenda, E., Harding, S. D., Pawson, A. J., Southan, C., Davies, J. A., Aldrich, R. W., Attali, B., Baggetta, A. M., Becirovic, E., Biel, M., Bill, R. M., Catterall, W. A., … Zhu, M. (2021). THE CONCISE GUIDE TO PHARMACOLOGY 2021/22: Ion channels. *British Journal of Pharmacology*, *178*(S1), S157–S245. https://doi.org/10.1111/bph.15539

Alexander, S. P. H., Roberts, R. E., Broughton, B. R. S., Sobey, C. G., George, C. H., Stanford, S. C., … Ahluwalia, A. (2018). Goals and practicalities of immunoblotting and immunohistochemistry: A guide for submission to the *British Journal of Pharmacology*. *British Journal of Pharmacology*, *175*, 407–411. https://doi.org/10.1111/bph.14112

Bennett, G. J., & Xie, Y. K. (1988). A peripheral mononeuropathy in rat that produces disorders of pain sensation like those seen in man. *Pain*, *33*, 87–107. https://doi.org/10.1016/0304-3959(88)90209-6

Bessac, B. F., Sivula, M., Von Hehn, C. A., Escalera, J., Cohn, L., & Jordt, S. E. (2008). TRPA1 is a major oxidant sensor in murine airway sensory neurons. *Journal of Clinical Investigation*, *118*, 1899–1910. https://doi.org/10.1172/JCI34192

Bhattacharya, M. R., Bautista, D. M., Wu, K., Haeberle, H., Lumpkin, E. A., & Julius, D. (2008). Radial stretch reveals distinct populations of mechanosensitive mammalian somatosensory neurons. *Proceedings of the National Academy of Sciences of the United States of America*, *105*, 20015–20020. https://doi.org/10.1073/pnas.0810801105

Bonet, I. J., Fischer, L., Parada, C. A., & Tambeli, C. H. (2013). The role of transient receptor potential A 1 (TRPA1) in the development and maintenance of carrageenan-induced hyperalgesia. *Neuropharmacology*, *65*, 206–212. https://doi.org/10.1016/j.neuropharm.2012.09.020

Chaplan, S. R., Bach, F. W., Pogrel, J. W., Chung, J. M., & Yaksh, T. L. (1994). Quantitative assessment of tactile allodynia in the rat paw. *Journal of Neuroscience Methods*, *53*, 55–63. https://doi.org/10.1016/0165-0270(94)90144-9

Curtis, M. J., Alexander, S. P. H., Cirino, G., George, C. H., Kendall, D. A., Insel, P. A., Izzo, A. A., Ji, Y., Panettieri, R. A., Patel, H. H., Sobey, C. G., Stanford, S. C., Stanley, P., Stefanska, B., Stephens, G. J., Teixeira, M. M., Vergnolle, N., & Ahluwalia, A. (2022). Planning experiments: Updated guidance on experimental design and analysis and their reporting III. *British Journal of Pharmacology*, *179*, 1–7. https://doi.org/10.1111/bph.15868

De Logu, F., de Prá, S. D. T., de David Antoniazzi, C. T., Kudsi, S. Q., Ferro, P. R., Landini, L., Rigo, F. K., de Bem Silveira, G., Silveira, P. C. L., Oliveira, S. M., Marini, M., Mattei, G., Ferreira, J., Geppetti, P., Nassini, R., & Trevisan, G. (2020). Macrophages and Schwann cell TRPA1 mediate chronic allodynia in a mouse model of complex regional pain syndrome type I. *Brain, Behavior, and Immunity*, *88*, 535–546. https://doi.org/10.1016/j.bbi.2020.04.037

De Logu, F., & Geppetti, P. (2019). Ion channel pharmacology for pain modulation. *Handbook of Experimental Pharmacology*, *260*, 161–186. https://doi.org/10.1007/164_2019_336

De Logu, F., Li Puma, S., Landini, L., Portelli, F., Innocenti, A., de Araujo, D. S. M., Janal, M. N., Patacchini, R., Bunnett, N. W., Geppetti, P., & Nassini, R. (2019). Schwann cells expressing nociceptive channel TRPA1 orchestrate ethanol-evoked neuropathic pain in mice. *The Journal of Clinical Investigation*, *129*, 5424–5441. https://doi.org/10.1172/JCI128022

De Logu, F., Marini, M., Landini, L., Souza Monteiro de Araujo, D., Bartalucci, N., Trevisan, G., Bruno, G., Marangoni, M., Schmidt, B. L., Bunnett, N. W., Geppetti, P., & Nassini, R. (2021). Peripheral nerve resident macrophages and Schwann cells mediate cancer-induced pain. *Cancer Research*, *81*, 3387–3401. https://doi.org/10.1158/0008-5472.CAN-20-3326

De Logu, F., Nassini, R., Hegron, A., Landini, L., Jensen, D. D., Latorre, R., Ding, J., Marini, M., Souza Monteiro de Araujo, D., Ramírez-Garcia, P., Whittaker, M., Retamal, J., Titiz, M., Innocenti, A., Davis, T. P., Veldhuis, N., Schmidt, B. L., Bunnett, N. W., & Geppetti, P. (2022). Schwann cell endosome CGRP signals elicit periorbital mechanical allodynia in mice. *Nature Communications*, *13*, 646. https://doi.org/10.1038/s41467-022-28204-z

De Logu, F., Nassini, R., Materazzi, S., Carvalho Gonçalves, M., Nosi, D., Rossi Degl'Innocenti, D., Marone, I. M., Ferreira, J., Li Puma, S., Benemei, S., Trevisan, G., Souza Monteiro de Araújo, D., Patacchini, R., Bunnett, N. W., & Geppetti, P. (2017). Schwann cell TRPA1 mediates neuroinflammation that sustains macrophage-dependent neuropathic pain in mice. *Nature Communications*, *8*, 1887. https://doi.org/10.1038/s41467-017-01739-2

Dixon, W. J. (1980). Efficient analysis of experimental observations. *Annual Review of Pharmacology and Toxicology*, *20*, 441–462. https://doi.org/10.1146/annurev.pa.20.040180.002301

Edvinsson, L., Haanes, K. A., Warfvinge, K., & Krause, D. N. (2018). CGRP as the target of new migraine therapies—Successful translation from bench to clinic. *Nature Reviews. Neurology*, *14*, 338–350. https://doi.org/10.1038/s41582-018-0003-1

Eid, S. R., Crown, E. D., Moore, E. L., Liang, H. A., Choong, K. C., Dima, S., Henze, D. A., Kane, S. A., & Urban, M. O. (2008). HC-030031, a TRPA1 selective antagonist, attenuates inflammatory- and neuropathy-induced mechanical hypersensitivity. *Molecular Pain*, *4*(1), 48.

Faul, F., Erdfelder, E., Lang, A. G., & Buchner, A. (2007). G*power 3: A flexible statistical power analysis program for the social, behavioral, and biomedical sciences. *Behavior Research Methods*, *39*, 175–191. https://doi.org/10.3758/BF03193146

Geppetti, P., & Holzer, P. (1996). *Neurogenic inflammation*. United States.

Hinman, A., Chuang, H. H., Bautista, D. M., & Julius, D. (2006). TRP channel activation by reversible covalent modification. *Proceedings of the National Academy of Sciences of the United States of America*, *103*, 19564–19568. https://doi.org/10.1073/pnas.0609598103

Jain, S. M., Balamurugan, R., Tandon, M., Mozaffarian, N., Gudi, G., Salhi, Y., Holland, R., Freeman, R., & Baron, R. (2022). Randomized, double-blind, placebo-controlled trial of ISC 17536, an oral inhibitor of transient receptor potential ankyrin 1, in patients with painful diabetic peripheral neuropathy: Impact of preserved small nerve fiber function. *Pain*, *163*, e738–e747. https://doi.org/10.1097/j.pain.0000000000002470

Jin, Y., Smith, C., Monteith, D., Brown, R., Camporeale, A., McNearney, T. A., Deeg, M. A., Raddad, E., Xiao, N., de la Peña, A., Kivitz, A. J., & Schnitzer, T. J. (2018). CGRP blockade by galcanezumab was not associated with reductions in signs and symptoms of knee osteoarthritis in a randomized clinical trial. *Osteoarthritis and Cartilage*, *26*, 1609–1618. https://doi.org/10.1016/j.joca.2018.08.019

Kilkenny, C., Browne, W. J., Cuthill, I. C., Emerson, M., & Altman, D. G. (2010). Improving bioscience research reporting: The ARRIVE guidelines for reporting animal research. *PLoS Biology*, *8*, e1000412. https://doi.org/10.1371/journal.pbio.1000412

LaMotte, R. H., Lundberg, L. E., & Torebjörk, H. E. (1992). Pain, hyperalgesia and activity in nociceptive C units in humans after intradermal injection of capsaicin. *The Journal of Physiology*, *448*, 749–764. https://doi.org/10.1113/jphysiol.1992.sp019068

Lewis, T. (1936). Experiments relating to cutaneous hyperalgesia and its spread through somatic nerves. *Clinical Science*, *2*, 373–414.

Lilley, E., Stanford, S. C., Kendall, D. E., Alexander, S. P. H., Cirino, G., Docherty, J. R., George, C. H., Insel, P. A., Izzo, A. A., Ji, Y., Panettieri, R. A., Sobey, C. G., Stefanska, B., Stephens, G., Teixeira, M., & Ahluwalia, A. (2020). ARRIVE 2.0 and the British Journal of Pharmacology: Updated guidance for 2020. *British Journal of Pharmacology*, *177*, 3611–3616. https://doi.org/10.1111/bph.15178

Ma, W., & Bisby, M. A. (2000). Calcitonin gene-related peptide, substance P and protein gene product 9.5 immunoreactive axonal fibers in the rat footpad skin following partial sciatic nerve injuries. *Journal of Neurocytology*, *29*(4), 249–262. https://doi.org/10.1023/A:1026519720352

Macpherson, L. J., Dubin, A. E., Evans, M. J., Marr, F., Schultz, P. G., Cravatt, B. F., & Patapoutian, A. (2007). Noxious compounds activate TRPA1 ion channels through covalent modification of cysteines. *Nature*, *445*, 541–545. https://doi.org/10.1038/nature05544

McNamara, C. R., Mandel-Brehm, J., Bautista, D. M., Siemens, J., Deranian, K. L., Zhao, M., Hayward, N. J., Chong, J. A., Julius, D., Moran, M. M., & Fanger, C. M. (2007). TRPA1 mediates formalin-induced pain. *Proceedings of the National Academy of Sciences of the United States of America*, *104*, 13525–13530. https://doi.org/10.1073/pnas.0705924104

Nassini, R., Materazzi, S., Benemei, S., & Geppetti, P. (2014). The TRPA1 channel in inflammatory and neuropathic pain and migraine. *Reviews of Physiology, Biochemistry and Pharmacology*, *167*, 1–43. https://doi.org/10.1007/112_2014_18

Percie du Sert, N., Hurst, V., Ahluwalia, A., Alam, S., Avey, M. T., Baker, M., Browne, W. J., Clark, A., Cuthill, I. C., Dirnagl, U., Emerson, M., Garner, P., Holgate, S. T., Howells, D. W., Karp, N. A., Lazic, S. E., Lidster, K., MacCallum, C. J., Macleod, M., … Würbel, H. (2020). The ARRIVE guidelines 2.0: Updated guidelines for reporting animal research. *PLoS Biology*, *18*(7), e3000410. https://doi.org/10.1371/journal.pbio.3000410

Petrus, M., Peier, A. M., Bandell, M., Hwang, S. W., Huynh, T., Olney, N., Jegla, T., & Patapoutian, A. (2007). A role of TRPA1 in mechanical hyperalgesia is revealed by pharmacological inhibition. *Molecular Pain*, *3*, 40.

Qiao, Z., Qi, H., Zhang, H., Zhou, Q., Wei, N., Zhang, Y., & Wang, K. W. (2020). Visualizing TRPA1 in the plasma membrane for rapidly screening optical control agonists via a photochromic ligand based fluorescent probe. *Analytical Chemistry*, *92*, 1934–1939. https://doi.org/10.1021/acs.analchem.9b04193

Reese, R. M., Dourado, M., Anderson, K., Warming, S., Stark, K. L., Balestrini, A., Suto, E., Lee, W., Riol-Blanco, L., Shields, S. D., & Hackos, D. H. (2020). Behavioral characterization of a CRISPR-generated TRPA1 knockout rat in models of pain, itch, and asthma. *Scientific Reports*, *10*, 979. https://doi.org/10.1038/s41598-020-57936-5

Russell, F. A., King, R., Smillie, S. J., Kodji, X., & Brain, S. D. (2014). Calcitonin gene-related peptide: Physiology and pathophysiology. *Physiological Reviews*, *94*, 1099–1142. https://doi.org/10.1152/physrev.00034.2013

Seltzer, Z., Dubner, R., & Shir, Y. (1990). A novel behavioral model of neuropathic pain disorders produced in rats by partial sciatic nerve injury. *Pain*, *43*(2), 205–218. https://doi.org/10.1016/0304-3959(90)91074-S

Sinclair, S. R., Kane, S. A., van der Schueren, B. J., Xiao, A., Willson, K. J., Boyle, J., de Lepeleire, I., Xu, Y., Hickey, L., Denney, W. S., Li, C. C., Palcza, J., Vanmolkot, F. H. M., Depré, M., van Hecken, A., Murphy, M. G., Ho, T. W., & de Hoon, J. N. (2010). Inhibition of capsaicin-induced increase in dermal blood flow by the oral CGRP receptor antagonist, telcagepant (MK-0974). *British Journal of Clinical Pharmacology*, *69*(1), 15–22. https://doi.org/10.1111/j.1365-2125.2009.03543.x

Story, G. M., Peier, A. M., Reeve, A. J., Eid, S. R., Mosbacher, J., Hricik, T. R., Earley, T. J., Hergarden, A. C., Andersson, D. A., Hwang, S. W., McIntyre, P., Jegla, T., Bevan, S., & Patapoutian, A. (2003). ANKTM1, a TRP-like channel expressed in nociceptive neurons, is activated by cold temperatures. *Cell*, *112*, 819–829. https://doi.org/10.1016/S0092-8674(03)00158-2

Szallasi, A., & Blumberg, P. M. (1999). Vanilloid (capsaicin) receptors and mechanisms. *Pharmacological Reviews*, *51*, 159–212.

Talavera, K., Startek, J. B., Alvarez-Collazo, J., Boonen, B., Alpizar, Y. A., Sanchez, A., Naert, R., & Nilius, B. (2020). Mammalian transient receptor potential TRPA1 channels: From structure to disease. *Physiological Reviews*, *100*, 725–803. https://doi.org/10.1152/physrev.00005.2019

Tao, Y. (2013). Isolation and culture of Schwann cells. *Methods in Molecular Biology*, *1018*, 93–104. https://doi.org/10.1007/978-1-62703-444-9_9

Trevisan, G., Hoffmeister, C., Rossato, M. F., Oliveira, S. M., Silva, M. A., Silva, C. R., Fusi, C., Tonello, R., Minocci, D., Guerra, G. P., Materazzi, S., Nassini, R., Geppetti, P., & Ferreira, J. (2014). TRPA1 receptor stimulation by hydrogen peroxide is critical to trigger hyperalgesia and inflammation in a model of acute gout. *Free Radical Biology & Medicine*, *72*, 200–209. https://doi.org/10.1016/j.freeradbiomed.2014.04.021

Van Steenwinckel, J., Auvynet, C., Sapienza, A., Reaux-Le Goazigo, A., Combadière, C., & Melik Parsadaniantz, S. (2015). Stromal cell-derived CCL2 drives neuropathic pain states through myeloid cell infiltration in injured nerve. *Brain, Behavior, and Immunity*, *45*, 198–210. https://doi.org/10.1016/j.bbi.2014.10.016

Wei, H., Hämäläinen, M. M., Saarnilehto, M., Koivisto, A., & Pertovaara, A. (2009). Attenuation of mechanical hypersensitivity by an antagonist of the TRPA1 ion channel in diabetic animals. *Anesthesiology*, *111*, 147–154. https://doi.org/10.1097/ALN.0b013e3181a1642b

SUPPORTING INFORMATION

Additional supporting information can be found online in the Supporting Information section at the end of this article.

How to cite this article: De Logu, F., De Siena, G., Landini, L., Marini, M., Souza Monteiro de Araujo, D., Albanese, V., Preti, D., Romitelli, A., Chieca, M., Titiz, M., Iannone, L. F., Geppetti, P., & Nassini, R. (2023). Non-neuronal TRPA1 encodes mechanical allodynia associated with neurogenic inflammation and partial nerve injury in rats. *British Journal of Pharmacology*, *180*(9), 1232–1246. https://doi.org/10.1111/bph.16005